



Global dynamics and optimal control of a nonlinear fractional-order cholera model

Anupam Khatua^{a,1} , Tapan Kumar Kar^b , Soovoojeet Jana^b 

^aDepartment of Applied Sciences and Humanities,
National Institute of Advanced Manufacturing Technology,
Ranchi, Jharkhand-834003, India
akhatua06@gmail.com

^bDepartment of Mathematics,
Indian Institute of Engineering Science and Technology,
Shibpur, Howrah-711103, West Bengal, India
tkar1117@gmail.com

^cDepartment of Mathematics, Ramsaday College,
Amta, Howrah-711401, West Bengal, India
soovoojeet@gmail.com

Received: December 21, 2022 / **Revised:** November 23, 2023 / **Published online:** January 15, 2024

Abstract. In this article, a fractional-order epidemic model for cholera is proposed and analyzed. Two transmission routes for cholera are considered to develop the compartmental epidemic model. The basic biological properties of the solutions of the fractional-order model are investigated. The global asymptotic stability of the equilibrium points have been established using appropriate Lyapunov functional. Moreover, a fractional-order control problem is presented, and its analytical solution is derived using Pontryagin's maximum principle. Also, some graphical visualizations of the theoretical results are provided. It is found that the fractional-order derivative only affect the time to reach the stationary states. Sensitivity analysis reveals that by reducing the rates of new recruitment and both the disease transmission rates, it may be possible to reduce the value of the basic reproduction number.

Keywords: cholera model, fractional-order derivative, global stability, Lyapunov functional, fractional optimal control.

1 Introduction

Cholera is considered as a major water borne disease caused by the bacteria *Vibrio Cholerae*. Generally, it takes 12 hours to 5 days to show symptoms after ingesting the contaminated food or water. It causes mainly diarrhea, vomiting and leg cramps. Although, the high income developed countries has been able to eradicate the cholera transmission due

¹Corresponding author.

to their better sanitation facilities. However, millions of people of under-developed and developing countries got affected by this bacterial disease due to the poor sanitation infrastructure and unavailability of hygienic drinking water. It has been estimated by the researchers that nearly 1.3 million to 4 million cases of cholera and 21000 to 143000 deaths due to cholera occur worldwide annually [35]. Moreover, in 2017, the Global Task Force on Cholera Control (GTFCC) had taken a strategy to reduce the deaths due to cholera by 90% [35]. Therefore, research works on the transmission process and control of cholera are very necessary and of great practical importance.

In last few decades, mathematical modelling is applied to predict the future dynamics of various emerging and reemerging infectious diseases. The results obtained from the model based studies have been used to guide the public health administrations and policy makers. The pioneering work of Kermack and McKendrick [10] is considered as the standard framework of the mathematical epidemiology. After that, numerous types of epidemic models have been developed incorporating many biological phenomena such as delay, age-structure, mobility, seasonality, spatial-heterogeneity etc. Some of those study can be found in [9, 11–13, 21] and the references cited therein. Several types of compartmental mathematical models have been also applied to understand the transmission mechanisms of cholera. Paio et al. [14] studied an SIQRB (susceptible-infectious-quarantine-recovered)-type model with a class of bacterial concentration. Also, they proposed and solved an optimal control problem in their system. Sun et al. [27] formulated a compartmental model for cholera that includes both person-to-person transmission and environment-to-person transmission. As an application of their work, they calculated the basic reproduction number in China. Wang et al. [31] presented a ODE-based cholera model first, incorporating the human behavior, and then they focused on a reaction–diffusion-type model considering the movement of humans and bacteria. They mainly investigated the spreading speed of cholera. Many other compartmental-type models using classical integer-order derivative can be found in [28, 33, 34] and the references therein. It is to be noted that all these systems are modeled by using integer-order derivatives.

Fractional calculus is a generalized version of the integer-order calculus. It has been used extensively in last few decades in different branches of sciences and technology [24], including electronic circuit analysis, control theory, heat transfer, fluid dynamics. The main motivation for using the fractional derivative is that it can incorporate memory, and most of the biological systems are equipped with memory. Moreover, the fractional-order derivative possesses nonlocal property. Also, fractional-order derivative enlarges the stability region of the dynamical systems. In last few years, it is being used immensely to solve many biological problems. Fractional-order differential equations are utilized to model the problems. In this context, we may refer some works in which fractional-order derivatives has been used to model and study the transmission of different types of diseases other than cholera (see [17, 22, 32]). Almedia [1] formulated a SEIR-type epidemic model using fractional-order derivatives. Torres et al. [26] studied the uniform asymptotic stability of a fractional-order model of tuberculosis. Huo et al. [7] presented a model of HIV with fractional derivatives and shown the influence of vaccination on occurring backward bifurcation. Several works with fractional derivatives can be found in literature [3, 8, 18, 20, 26, 32]. Motivated by those works, we propose a fractional-order

epidemic model to study the dynamical behavior of cholera. The remaining of this article is as follows.

In Section 2, the model is developed considering the transmission paths of cholera. The dynamical behavior of the system including the existence and uniqueness of the solutions and stability analysis of the model system are discussed in Section 3. A fractional-order control problem is framed and solved analytically in Section 4. In Section 5, effects of model parameters on the basic reproduction is studied. Also, some numerical simulations of the theoretical results are provided in Section 6. Finally, in Section 7, this article comes to an end with some conclusions.

2 Model formulation

Here we formulate a fractional-order compartmental model to analyze the transmission dynamics of cholera. Both the direct and indirect routes of transmission and fractional-order derivatives have been considered to model the system. We consider three compartments, namely, the susceptible group S , the infected group I and the recovered group R for the total human population, and also, another compartment is considered for the bacterial concentration B . Two major transmission paths of cholera are considered: human-to-human and environment-to-human. As a result, two transmission rates are taken. The constants β_h and β_e stand for the human-to-human and environment-to-human transmissions, respectively. Bilinear incidence rates are considered for both types of transmission, and γ is taken as the recovery rate of the infected individuals. The positive constant A is taken as the recruitment rate to the susceptible class, and $\mu (> 0)$, δ are natural and disease related death rate, respectively. Also, when the number of infected individuals increases, then the bacterial concentration also increases. Let σ denotes the bacterial concentration rate contributed by the each infected individual, and d denotes diminishing rate of bacteria.

Based on these assumptions and utilizing fractional-order derivative in Caputo sense, we write down the following system for the transmission of cholera:

$$\begin{aligned} D_t^\alpha S &= A - \beta_h SI - \beta_e SB - \mu S, \\ D_t^\alpha I &= \beta_h SI + \beta_e SB - (\gamma + \mu + \delta)I, \\ D_t^\alpha R &= \gamma I - \mu R, \\ D_t^\alpha B &= \sigma I - dB, \end{aligned}$$

where D_t^α denotes Caputo fractional derivative, and $\alpha \in (0, 1]$. The Caputo fractional derivative of order α is defined as

$$D_t^\alpha f(t) = \frac{1}{\Gamma(n - \alpha)} \int_0^t (t - s)^{n-\alpha-1} f^{(n)}(s) ds,$$

$n - 1 < \alpha < n$, $n \in \mathbb{N}$, and if $\alpha = n \in \mathbb{N}$, then $D_t^\alpha f(t) = f^{(n)}(t)$ [2]. The advantage of using Caputo’s definition is that the initial conditions for both the fractional-order differential equation with Caputo derivative and integer differential equation are same.

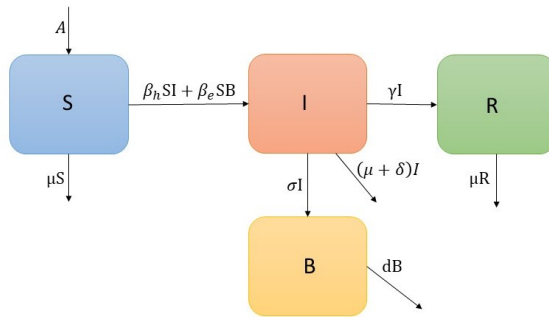


Figure 1. Schematic diagram representing the disease transmission.

We consider the initial values as $S(0) > 0, I(0) > 0, R(0) > 0, B(0) > 0$. The disease transmission scenario is presented in Fig. 1.

It is easy to note that the equations corresponding to state variables S, I and B are independent of R . So it is equivalent to study the following subsystem:

$$\begin{aligned}
 D_t^\alpha S &= A - \beta_h SI - \beta_e SB - \mu S, \\
 D_t^\alpha I &= \beta_h SI + \beta_e SB - (\gamma + \mu + \delta)I, \\
 D_t^\alpha B &= \sigma I - dB,
 \end{aligned}
 \tag{1}$$

where the initial values are same as earlier.

3 Dynamical analysis

3.1 Basic properties of the solutions

Theorem 1. *There is a unique solution of model (1).*

Proof. Denote $X(t) = (S, I, B) = (x_1, x_2, x_3)^T$. Then model (1) becomes

$$D_t^\alpha X(t) = A_1 X(t) + x_1 A_2 X(t) + A_3,$$

where

$$A_1 = \begin{pmatrix} -\mu & 0 & 0 \\ 0 & -(\mu + \gamma + \delta) & 0 \\ 0 & \sigma & -d \end{pmatrix}, \quad A_2 = \begin{pmatrix} 0 & -\beta_h & -\beta_e \\ 0 & \beta_h & \beta_e \\ 0 & 0 & 0 \end{pmatrix} \quad \text{and} \quad A_3 = \begin{pmatrix} A \\ 0 \\ 0 \end{pmatrix}.$$

Let us denote $\Gamma(t, X(t)) = A_1 X(t) + x_1 A_2 X(t) + A_3$. Now

$$\begin{aligned}
 &\|\Gamma(t, X(t)) - \Gamma(t, Y(t))\| \\
 &= \|(A_1 X(t) + x_1 A_2 X(t) + A_3) - (A_1 Y(t) + x_1 A_2 Y(t) + A_3)\| \\
 &= \|A_1(X(t) - Y(t)) + x_1 A_2(X(t) - Y(t))\| \\
 &= \|(A_1 + x_1 A_2)(X(t) - Y(t))\| \leq L\|(X(t) - Y(t))\|,
 \end{aligned}$$

where $L = \max(A_1 + x_1 A_2)$, the norm $\|\cdot\|$ denotes the usual Euclidean norm, and the complete normed space is the 3-dimensional Euclidean space.

Therefore, $\Gamma(X)$ satisfies the Lipschitz condition, and hence, following the work of Diethelm and Ford [5], we conclude that the system has a unique solution. \square

Theorem 2. *All the solutions of model (1) are nonnegative and uniformly bounded.*

Proof. From our proposed model (1) we have

$$\begin{aligned} D_t^\alpha S|_{S=0} &= A \geq 0, \\ D_t^\alpha I|_{I=0} &= \beta_e S B \geq 0, \\ D_t^\alpha B|_{B=0} &= \sigma I \geq 0. \end{aligned}$$

Hence, it follows from the work of Odibat and Shawagfeh [23] that all the solutions will always remain in \mathbb{R}_+^3 .

Assuming $N(t) = S(t) + I(t)$ and adding first two equations of (1), we get

$$\begin{aligned} D_t^\alpha N &= A - \mu(S + I) - (\gamma + \delta)I \\ &= A - \mu N - (\gamma + \delta)I \\ &\leq A - \mu N. \end{aligned}$$

Now integrating and using the Lemma 3 of [15], we have

$$N(t) \leq \frac{A}{\mu} + \left(-\frac{A}{\mu} + N(0)\right) E_\alpha(-\mu t^\alpha).$$

Here E_α denotes the Mittag-Leffler function.

Thus, $N(t) \rightarrow A/\mu$ when $t \rightarrow \infty$, and hence $0 < N(t) \leq A/\mu$.

Also, from the last equation of (1) we get

$$D_t^\alpha B = \sigma I - dB \leq \sigma \frac{A}{\mu} - dB,$$

i.e.,

$$D_t^\alpha B + dB \leq \frac{A\sigma}{\mu}.$$

Now using the Lemma 3 of [15], we get

$$B(t) \leq \left(B(0) - \frac{\sigma A}{\mu d}\right) E_\alpha(-dt^\alpha) + \frac{\sigma A}{\mu d}.$$

Thus, $B(t) \rightarrow \sigma A/\mu d$ when $t \rightarrow \infty$, and hence $0 < B(t) \leq \sigma A/(\mu d)$.

Therefore, all the solutions originating in \mathbb{R}_+^3 are restricted in the domain $\Omega_H \times \Omega_B$, where

$$\Omega_H = \left\{ (S, I) \mid 0 \leq S + I \leq \frac{A}{\mu} \right\} \quad \text{and} \quad \Omega_B = \left\{ B \mid 0 \leq B \leq \frac{\sigma A}{\mu d} \right\}. \quad \square$$

3.2 Equilibria and stability analysis

In order to investigate the dynamics of the proposed system, first, we have derived the expression of basic reproduction number following the next generation matrix method [29]. The basic reproduction number of system (1) is obtained as

$$R_0 = \frac{A(\beta_h d + \beta_e \sigma)}{\mu d(\gamma + \mu + \delta)}.$$

Now the equilibrium points of system (1) are obtained as a solution of the following system of simultaneous equations:

$$D_t^\alpha S = 0, \quad D_t^\alpha I = 0, \quad D_t^\alpha B = 0.$$

Thus, we get two equilibrium points, namely, disease free equilibrium $E_0 = (S^0, 0, 0) = (A/\mu, 0, 0)$ and endemic equilibrium $E_1(S^*, I^*, B^*)$, where

$$S^* = \frac{d(\gamma + \mu + \delta)}{\beta_h d + \beta_e \sigma}, \quad I^* = \frac{\mu d}{\beta_h d + \beta_e \sigma}(R_0 - 1) \quad \text{and} \quad B^* = \frac{\sigma I^*}{d}.$$

It is easy to observe that the infected equilibrium point exist only when $R_0 > 1$.

Now the stability of the equilibria E_0 and E_1 have been studied.

Theorem 3. *The disease-free equilibrium point E_0 of the fractional-order system (1) is locally asymptotically stable if $R_0 < 1$.*

Proof. The Jacobian matrix of (1) at $E_0(A/\mu, 0, 0)$ is

$$J(E_0) = \begin{pmatrix} -\mu & \frac{-\beta_h A}{\mu} & \frac{-\beta_e A}{\mu} \\ 0 & \frac{\beta_h A}{\mu} - \gamma - \mu - \delta & \frac{\beta_e A}{\mu} \\ 0 & \sigma & -d \end{pmatrix}.$$

Therefore, the characteristic equation of the system at E_0 is

$$(s + \mu) \left[s^2 + \left(\mu + \gamma + \delta + d - \frac{\beta_h A}{\mu} \right) s + (\gamma + \mu + \delta)d - \frac{A}{\mu}(\beta_h d + \beta_e \sigma) \right] = 0.$$

Now one root of the above equation is $s_1 = -\mu$, and the remaining two roots s_2, s_3 are solution of the following equation:

$$s^2 + \left(\mu + \gamma + \delta + d - \frac{\beta_h A}{\mu} \right) s + (\gamma + \mu + \delta)d - \frac{A}{\mu}(\beta_h d + \beta_e \sigma) = 0. \quad (2)$$

Now when $R_0 < 1$, we observe that

$$s_2 + s_3 = \frac{\beta_h A}{\mu} - \mu - \gamma - \delta - d < 0,$$

$$s_2 s_3 = (\gamma + \mu + \delta)d - \frac{A}{\mu}(\beta_h d + \beta_e \sigma) > 0.$$

Hence, the roots of Eq. (2) have negative real parts. So, we observe that $|\arg(s_i)| > \alpha\pi/2$ for all $\alpha \in (0, 1]$, $i = 1, 2, 3$. Therefore, we conclude that the infection-free equilibrium point of the system is locally asymptotically stable when $R_0 < 1$. \square

Now the Jacobian matrix of (1) evaluated at E_1 is

$$J(E_1) = \begin{pmatrix} -\beta_e B^* - \beta_h I^* - \mu & -\beta_h S^* & -\beta_e S^* \\ \beta_e B^* + \beta_h I^* & \beta_h S^* - \gamma - \mu - \delta & \beta_e S^* \\ 0 & \sigma & -d \end{pmatrix}.$$

The characteristics equation at E_1 is

$$f(\psi) = \psi^3 + r_1\psi^2 + r_2\psi + r_3 = 0, \quad (3)$$

where

$$\begin{aligned} r_1 &= \beta_e B^* + \beta_h I^* + \gamma + d + 2\mu + \delta - \beta_h S^*, \\ r_2 &= (\gamma + 2\mu + \delta + \beta_e B^* + \beta_h I^*)d \\ &\quad + (\gamma + \mu + \delta - \beta_h S^*)(\beta_e B^* + \beta_h I^* + \mu) \\ &\quad + \beta_h S^*(\beta_e B^* + \beta_h I^*) - (\beta_h d + \beta_e \sigma)S^*, \\ r_3 &= S^*(\beta_h d + \beta_e \sigma)(\beta_e B^* + \beta_h I^*) \\ &\quad - (\beta_e B^* + \beta_h I^* + \mu)\{\beta_e \sigma S^* + d(\beta_h S^* - \gamma - \mu - \delta)\}. \end{aligned}$$

Let $D(f)$ denote the discriminant of the polynomial $f(\psi)$, and it is given by

$$D(f) = \begin{vmatrix} 1 & r_1 & r_2 & r_3 & 0 \\ 0 & 1 & r_1 & r_2 & r_3 \\ 3 & 2r_1 & r_2 & 0 & 0 \\ 0 & 3 & 2r_1 & r_2 & 0 \\ 0 & 0 & 3 & 2r_1 & r_2 \end{vmatrix} = 18r_1r_2r_3 + (r_1r_2)^2 - 4r_3r_1^3 - 4r_2^3 - 27r_3^2.$$

Now we get the following theorem.

Theorem 4. Suppose that E_1 exists in \mathbb{R}_+^3 . Then

- (i) If $D(f) > 0$, $r_1 > 0$, $r_3 > 0$, and $r_1r_2 > r_3$, then for all $\alpha \in (0, 1]$, E_1 is locally asymptotically stable.
- (ii) If $D(f) < 0$, $r_1 \geq 0$, $r_2 \geq 0$, $r_3 > 0$, and $0 < \alpha < 2/3$, then E_1 is locally asymptotically stable.
- (iii) If $D(f) < 0$, $r_1 < 0$, $r_2 < 0$, $\alpha > 2/3$, then E_1 is unstable.

Proof. (i) If $D(f) > 0$, then all the roots of Eq. (3) are real and distinct. If not, let us consider that Eq. (3) has one real root ψ_1 and two complex conjugate roots ψ_2, ψ_3 . Now, following [19], the discriminant is written as

$$D(f) = [(\psi_1 - \psi_2)(\psi_1 - \psi_3)(\psi_2 - \psi_3)]^2.$$

Now

$$\begin{aligned} & (\psi_1 - \psi_2)(\psi_1 - \psi_3)(\psi_2 - \psi_3) \\ &= (\psi_1 - \psi_2)(\psi_1 - \bar{\psi}_2)(\psi_2 - \bar{\psi}_2) = (\psi_1 - \psi_2)(\psi_1 - \bar{\psi}_2)2 \operatorname{Im}(\psi_2)i \\ &= (\psi_1 - \psi_2)\overline{(\psi_1 - \psi_2)}2 \operatorname{Im}(\psi_2)i = 2|\psi_1 - \psi_2|^2 \operatorname{Im}(\psi_2)i. \end{aligned}$$

Therefore,

$$D(f) = [2|\psi_1 - \psi_2|^2 \operatorname{Im}(\psi_2)i]^2 < 0,$$

which violates the condition that $D(f) > 0$. Thus, Eq. (3) has three distinct real roots whenever $D(f) > 0$. Now, due to $r_1 > 0, r_3 > 0$ and $r_1 r_2 > r_3$, all the roots of (3) are negative or have negative real parts. Since $D(f) > 0$, all roots of (3) are negative. As a result, $|\arg(\psi_i)| = \pi > \alpha\pi/2$ for all $\alpha \in (0, 1], i = 1, 2, 3$, and hence, E_1 is locally asymptotically stable.

(ii) In case (i), we have observed that for $D(f) < 0$, Eq. (3) has one real and two complex conjugate roots. Since $r_3 > 0$, so the real root is negative. We consider that the roots are $\psi_1 = -k(k > 0), \psi_{2,3} = \phi_1 \pm i\phi_2(\phi_1, \phi_2 \in R)$ and

$$f(\psi) = (\psi + k)(\psi - \phi_1 - i\phi_2)(\psi - \phi_1 + i\phi_2).$$

Comparing this with (3), we get $r_1 = k - 2\phi_1, r_2 = \phi_1^2 + \phi_2^2 - 2k\phi_1, r_3 = k(\phi_1^2 + \phi_2^2)$. Now $r_1 \geq 0$ implies $k > 2\phi_1$. Observing $\phi_1^2 \sec^2 \theta = \phi_1^2 + \phi_2^2$ and $r_2 \geq 0$, we get $\sec^2 \theta \geq 4$. So, $\theta = |\arg(\psi)| \geq \pi/3$. As $\alpha \in (0, 2/3)$, then $|\arg(\psi)| = \theta \geq \pi/3 > \alpha\pi/2$ holds good. Hence, all the roots of (3) satisfy $|\arg(\psi_i)| > \alpha\pi/2$ for all $\alpha \in (0, 1]$. So, E_1 is locally asymptotically stable.

Result (iii) can be proved in a similar way as (ii), and so we omit it. □

Now we aim to study the global asymptotic stability of the different equilibrium points. The lemma written below is employed, while proving the global stability of disease-free and endemic equilibrium.

Lemma 1. (See [30].) *Let $g(t) \in R^+$ be a continuous and derivable function. Then for any time $t \geq t_0$, we have*

$$D_t^\alpha \left(g(t) - g^*(t) - \ln \frac{g(t)}{g^*(t)} \right) \leq 1 - \frac{g^*(t)}{g(t)} D_t^\alpha g(t), \quad g^* \in R^+, \alpha \in (0, 1).$$

Theorem 5. *The infection free equilibrium is globally asymptotically stable if $R_0 < 1$.*

Proof. Let us consider the Lyapunov functional $W(t)$ as follows:

$$\begin{aligned} W(t) &= \frac{1}{\mu + \gamma + \delta} \left(S(t) - S^0 - S^0 \ln \frac{S(t)}{S^0} \right) + \frac{1}{\mu + \gamma + \delta} I(t) \\ &\quad + \frac{\beta_e S^0}{d(\mu + \gamma + \delta)} B(t). \end{aligned}$$

Now computing the fractional derivative of $W(t)$ and applying Lemma 1, we obtain

$$\begin{aligned}
 D_t^\alpha W(t) &\leq \frac{1}{\mu + \gamma + \delta} \left(1 - \frac{S^0}{S}\right) D_t^\alpha S(t) + \frac{1}{\mu + \gamma + \delta} D_t^\alpha I(t) \\
 &\quad + \frac{\beta_e S^0}{d(\mu + \gamma + \delta)} D_t^\alpha B(t) \\
 &= \frac{1}{\mu + \gamma + \delta} \left(1 - \frac{S^0}{S}\right) (A - \beta_h SI - \beta_e SB - \mu S) \\
 &\quad + \frac{1}{\mu + \gamma + \delta} (\beta_h SI + \beta_e SB - \gamma I - \mu I - \delta I) + \frac{\beta_e S^0}{d(\mu + \gamma + \delta)} (\sigma I - dB) \\
 &= \frac{1}{\mu + \gamma + \delta} \left(1 - \frac{S^0}{S}\right) \{\mu(S^0 - S) - \beta_h SI - \beta_e SB\} \\
 &\quad + \frac{1}{\mu + \gamma + \delta} (\beta_h SI + \beta_e SB - \gamma I - \mu I - \delta I) + \frac{\beta_e S^0}{d(\mu + \gamma + \delta)} (\sigma I - dB) \\
 &= \frac{-\mu}{S(\mu + \gamma + \delta)} (S - S^0)^2 + \left\{ \frac{\beta_e S^0 \sigma}{d(\mu + \gamma + \delta)} + \frac{\beta_h S^0}{\mu + \gamma + \delta} - 1 \right\} I \\
 &= \frac{-\mu}{S(\mu + \gamma + \delta)} (S - S^0)^2 + \left\{ \frac{A(\beta_h d + \beta_e \sigma)}{\mu d(\mu + \gamma + \delta)} - 1 \right\} I \\
 &= \frac{-\mu}{S(\mu + \gamma + \delta)} (S - S^0)^2 + (R_0 - 1)I.
 \end{aligned}$$

Observe that $D_t^\alpha W(t) = 0$ at $E_0 = (S_0, 0, 0) = (A/\mu, 0, 0)$, and $D_t^\alpha W(t) \leq 0$ if $R_0 < 1$. Hence, from LaSalle’s invariance principle it is concluded that the equilibrium point E_0 is globally asymptotically stable if $R_0 < 1$. \square

Theorem 6. *The infected steady state $E_1 = (S^*, I^*, B^*)$ is globally asymptotically stable if $R_0 > 1$.*

Proof. Consider the Lyapunov functional $V(t)$ as follows:

$$V(t) = V_1(S(t)) + V_2(I(t)) + \frac{\beta_e S^* B^*}{\sigma I^*} V_3(B(t)),$$

where

$$V_1 = S(t) - S^* - S^* \ln \frac{S(t)}{S^*},$$

$$V_2 = I(t) - I^* - I^* \ln \frac{I(t)}{I^*},$$

$$V_3 = B(t) - B^* - B^* \ln \frac{B(t)}{B^*}.$$

The above defined function $V(t)$ is continuously differentiable and positive definite for all $(S(t), I(t), B(t)) \neq (S^*, I^*, B^*)$, and $V(t) = 0$ when $(S(t), I(t), B(t)) = (S^*, I^*, B^*)$.

Now, computing the fractional derivative of $V(t)$ and applying Lemma 1, we obtain

$$\begin{aligned}
 D_t^\alpha V(t) &\leq \left(1 - \frac{S^*}{S}\right) D_t^\alpha S(t) + \left(1 - \frac{I^*}{I}\right) D_t^\alpha I(t) + \frac{\beta_e S^* B^*}{\sigma I^*} \left(1 - \frac{B^*}{B}\right) D_t^\alpha B(t) \\
 &= \left(1 - \frac{S^*}{S}\right) (A - \beta_h SI - \beta_e SB - \mu S) \\
 &\quad + \left(1 - \frac{I^*}{I}\right) (\beta_h SI + \beta_e SB - \gamma I - \mu I - \delta I) \\
 &\quad + \frac{\beta_e S^* B^*}{\sigma I^*} \left(1 - \frac{B^*}{B}\right) (\sigma I - dB) \\
 &= \left(1 - \frac{S^*}{S}\right) (\beta_h S^* I^* + \beta_e S^* B^* + \mu S^* - \beta_h SI - \beta_e SB - \mu S) \\
 &\quad + \left(1 - \frac{I^*}{I}\right) (\beta_h SI + \beta_e SB - \gamma I - \mu I - \delta I) \\
 &\quad + \frac{\beta_e S^* B^*}{\sigma I^*} \left(1 - \frac{B^*}{B}\right) (\sigma I - dB) \\
 &= \mu S^* \left(2 - \frac{S}{S^*} - \frac{S^*}{S}\right) + \beta_h S^* I^* \left(1 - \frac{S^*}{S} - \frac{S}{S^* I^*} + \frac{I}{I^*}\right) \\
 &\quad + \beta_e S^* B^* \left(1 - \frac{S^*}{S} - \frac{S}{S^* B^*} + \frac{B}{B^*}\right) \\
 &\quad + \left(1 - \frac{I^*}{I}\right) (\beta_h SI + \beta_e SB - \gamma I - \mu I - \delta I) \\
 &\quad + \frac{\beta_e S^* B^*}{\sigma I^*} \left(1 - \frac{B^*}{B}\right) (\sigma I - dB).
 \end{aligned}$$

At the endemic equilibrium, $(\gamma + \mu + \delta)I^* = \beta_e S^* B^* + \beta_h S^* I^*$. Using this and after some simplifications, we have

$$\begin{aligned}
 D_t^\alpha V(t) &\leq \mu S^* \left(2 - \frac{S}{S^*} - \frac{S^*}{S}\right) + \beta_h S^* I^* \left(1 - \frac{S^*}{S} - \frac{S}{S^*} + \frac{I}{I^*}\right) \\
 &\quad + \beta_e S^* B^* \left(1 - \frac{S^*}{S} - \frac{S}{S^* B^*} + \frac{B}{B^*}\right) \\
 &\quad - (\gamma + \mu + \delta)I + (\gamma + \mu + \delta)I^* + \frac{\beta_e S^* B^*}{\sigma I^*} \left(1 - \frac{B^*}{B}\right) (\sigma I - dB) \\
 &= \mu S^* \left(2 - \frac{S}{S^*} - \frac{S^*}{S}\right) + \beta_h S^* I^* \left(2 - \frac{S}{S^*} - \frac{S^*}{S}\right) \\
 &\quad + \beta_e S^* B^* \left(2 - \frac{S^*}{S} - \frac{I}{I^*} + \frac{B}{B^*} - \frac{S}{S^* B^*} + \frac{I}{I^*}\right) \\
 &\quad + \frac{\beta_e S^* B^*}{\sigma I^*} \left(1 - \frac{B^*}{B}\right) (\sigma I - dB).
 \end{aligned}$$

Moreover, using the relation $\sigma I^* - dB^* = 0$, we have

$$\begin{aligned}
 D_t^\alpha V(t) &\leq \mu S^* \left(2 - \frac{S}{S^*} - \frac{S^*}{S} \right) + \beta_h S^* I^* \left(2 - \frac{S}{S^*} - \frac{S^*}{S} \right) \\
 &\quad + \beta_e S^* B^* \left(2 - \frac{S^*}{S} - \frac{I}{I^*} + \frac{B}{B^*} - \frac{S}{S^*} \frac{B}{B^*} \frac{I^*}{I} \right) \\
 &\quad + \frac{\beta_e S^* B^*}{\sigma I^*} \left(\sigma I - dB - \frac{\sigma I B^*}{B} + \sigma I^* \right).
 \end{aligned}$$

Finally, using again the relation $\sigma I^* - dB^* = 0$ and after some simplifications, we obtain

$$\begin{aligned}
 D_t^\alpha V(t) &\leq \underbrace{\mu S^* \left(2 - \frac{S}{S^*} - \frac{S^*}{S} \right)}_I + \beta_h S^* I^* \underbrace{\left(2 - \frac{S}{S^*} - \frac{S^*}{S} \right)}_I \\
 &\quad + \underbrace{\beta_e S^* B^* \left(3 - \frac{S^*}{S} - \frac{I}{I^*} \frac{B^*}{B} - \frac{S}{S^*} \frac{B}{B^*} \frac{I^*}{I} \right)}_{II}.
 \end{aligned}$$

Now, since A.M. \geq G.M., we get $I \leq 0$ for $S > 0$, and $I = 0$ iff $S = S^*$; $II \leq 0$ if $S > 0, I > 0, B > 0$, and $II = 0$ iff $S = S^*, I = I^*, B = B^*$.

Hence, $D_t^\alpha V(t) \leq 0$ for all $S, I, B > 0$, and $D_t^\alpha V(t) = 0$ at (S^*, I^*, B^*) , so, the invariant set for the system in which $D_t^\alpha V(t) = 0$ is $\{(S^*, I^*, B^*)\}$. Hence, following LaSalle’s invariance principle, we conclude that the steady state E_1 is globally asymptotically stable if $R_0 > 1$. □

4 Fractional-order optimal control

In the last section, we have thoroughly analyzed the dynamical behavior of the system. But any kind of control measure for the infected persons is not considered. Now we wish to explore the situation when some treatment is given to the infectious individuals. So, we incorporate a control function $u(t)$ ($0 \leq u(t) \leq 1$) denoting treatment control into our model. We aim to minimize number of infected persons and associated treatment cost.

We consider the objective functional for the optimal control problem as follows:

$$\min J(I(t), u(t)) = \int_0^{t_f} (C_1 I(t) + C_2 u^2(t)) dt \tag{4}$$

subject to the system

$$\begin{aligned}
 D_t^\alpha S &= A - \beta_h SI - \beta_e SB - \mu S, \\
 D_t^\alpha I &= \beta_h SI + \beta_e SB - (\gamma + \mu + \delta)I - u(t)I, \\
 D_t^\alpha R &= \gamma I - \mu R + u(t)I, \\
 D_t^\alpha B &= \sigma I - dB
 \end{aligned}$$

with positive initial values.

Now we utilize Pontryagin's maximum principle [25] for fractional optimal control to solve above problem.

Theorem 7. Let the control variable $u(t)$ be measurable function in $[0, t_f]$ and bounded in $[0, 1]$. Then there is an optimal control u^* , which minimizes the objective functional J of (4) with

$$\begin{aligned} D_t^\alpha p_1(t) &= p_1(t)(\beta_h I + \beta_e B + \mu) - p_2(t)(\beta_h I + \beta_e B), \\ D_t^\alpha p_2(t) &= -C_1 + p_1(t)\beta_h S - p_2(t)\beta_h S + p_2(t)(\gamma + \mu + \delta + u(t)) \\ &\quad - p_3(t)(\gamma + u) - p_4(t)\sigma, \\ D_t^\alpha p_3(t) &= p_3(t)\mu, \\ D_t^\alpha p_4(t) &= p_4(t)d + p_1(t)\beta_e S - p_2(t)\beta_e S, \end{aligned}$$

where

$$u^* = \max \left\{ \min \left\{ \frac{(p_2(t) - p_3(t))I(t)}{2C_2}, 1 \right\}, 0 \right\}.$$

Proof. The Hamiltonian of our optimal control problem is

$$\begin{aligned} H &= C_1 I(t) + C_2 u^2(t) + p_1(A - \beta_h SI - \beta_e SB - \mu S) \\ &\quad + p_2(\beta_h SI + \beta_e SB - (\gamma + \mu + \delta) - u(t)I)I \\ &\quad + p_3(\gamma I - \mu R + u(t)I) + p_4(\sigma I - dB), \end{aligned}$$

where C_1, C_2 are the weight factors, and $p_i(t)$, $i = 1, 2, 3, 4$, are the adjoint variables, which satisfy the transversality conditions $p_i(t_f) = 0$, $i = 1(1)4$, and the adjoint variables are obtained as the solution of the following system of equations:

$$\begin{aligned} D_t^\alpha p_1(t) &= -\frac{\partial H}{\partial S} \\ &= p_1(t)(\beta_h I + \beta_e B + \mu) - p_2(t)(\beta_h I + \beta_e B), \\ D_t^\alpha p_2(t) &= -\frac{\partial H}{\partial I} \\ &= -C_1 + p_1(t)\beta_h S - p_2(t)\beta_h S + p_2(t)(\gamma + \mu + \delta + u(t)) \\ &\quad - p_3(t)(\gamma + u) - p_4(t)\sigma, \\ D_t^\alpha p_3(t) &= -\frac{\partial H}{\partial R} = p_3(t)\mu, \\ D_t^\alpha p_4(t) &= -\frac{\partial H}{\partial B} = p_4(t)d + p_1(t)\beta_e S - p_2(t)\beta_e S. \end{aligned}$$

Now, we are at the stage where the problem of obtaining u^* minimizing J is same as to minimizing the Hamiltonian with respect to u . Therefore, using Pontryagin's maximum

principle, the optimal condition is

$$\frac{\partial H}{\partial u} = 2C_2u - p_2(t)I(t) + p_3(t)I(t) = 0$$

that can be solved using the state and costate variables resulting $\bar{u} = (p_2(t) - p_3(t))I(t)/(2C_2)$.

Now, for the optimal value of the control u^* , we consider the restrictions of the control and the sign of $\partial H/\partial u$. So, we get

$$u^* = \begin{cases} 0 & \text{if } \frac{\partial H}{\partial u} < 0, \\ \bar{u} & \text{if } \frac{\partial H}{\partial u} = 0, \\ 1 & \text{if } \frac{\partial H}{\partial u} > 0, \end{cases}$$

and $u^* = \max\{\min\{\bar{u}, 1\}, 0\}$, where $\bar{u} = (p_2(t) - p_3(t))I(t)/(2C_2)$. □

5 Sensitivity analysis of R_0

In order to measure the impacts of the parameters on the system, we perform sensitivity analysis in this section. Sensitivity indices reflect whether the parameters have a positive or negative effect on the system. Here we have calculated the sensitivity indices of the parameters on the basic reproduction number following the work of Das et al. [4]. Also, we choose the parameters values as $A = 6, \beta_h = 0.08, \beta_e = 0.3, \mu = 0.3, \delta = 0.2, \gamma = 0.6, \sigma = 0.2, d = 0.7$. Following [4], we consider the following definition of sensitivity index.

Definition 1. The normalized forward sensitivity index of a variable A is denoted by $\Gamma_A^{R_0}$, and it is defined as

$$\Gamma_A^{R_0} = \frac{\partial R_0}{\partial A} \cdot \frac{A}{R_0}.$$

Sensitivity indices of the parameters are provided in Table 1. We note that the recruitment rate to the susceptible class A is the most positively sensitive parameter, while the natural mortality rate has the most negative impact on the basic reproduction number. In Fig. 2, the bar diagram of the sensitivity indices is shown.

Table 1. Sensitivity indices of the parameters associated to R_0 .

Parameters	Description of parameters	Sensitivity indices
A	Recruitment rate	+1
β_h	Human to human transmission rate	+0.4828
γ	Recovery rate from infected class	-0.5455
β_e	Environment to human transmission rate	+0.5172
δ	Death rate due to disease	-0.1818
d	Diminishing rate of bacteria	-0.5172
μ	Natural death rate	-1.0909
σ	Bacteria concentration rate	+0.5172

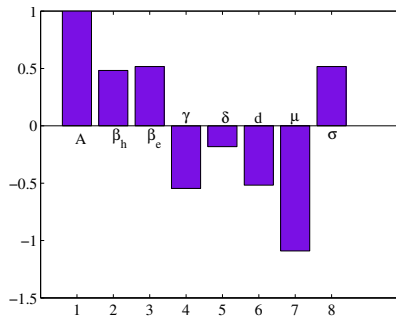


Figure 2. Bar diagram of the sensitivity indices of the parameters related to R_0 .

6 Numerical simulations

It is very essential to verify the analytical results numerically. The present section is composed with the simulations of system (1) and the fractional optimal control problem. It may also be noted that the simulations presented in this paper should be considered from a qualitative rather than a quantitative point of view. We have used *fimm2* MATLAB function to solve system (1) numerically. The function is based on some fractional linear multistep methods (FLMMs) of second order (see Garrappa [6] and Lubich [16]). Moreover, we have used the Euler’s forward–backward iterative scheme in MATLAB interface to solve the fractional control problem numerically. We have briefly described the process below. The fractional optimal control problem is a two-point boundary value problem consisting with a set of fractional-order differential equations. The system with the state variables is an initial value problem, whereas the system with the adjoint variables is a boundary value problem. We use forward iteration method to solve the state system and backward iteration method to the costate system.

The state system is solved using the following iterative scheme:

$$\begin{aligned}
 S(i) &= (A - \beta_h S(i-1)I(i-1) - \beta_e S(i)B(i) - \mu S(i))h^\alpha - \sum_{j=1}^i c(j)S(i-j), \\
 I(i) &= (\beta_h S(i)I(i-1) + \beta_e S(i)B(i-1) - (\gamma + \mu + \delta)I(i-1) - uI(i-1))h^\alpha \\
 &\quad - \sum_{j=1}^i c(j)I(i-j), \\
 R(i) &= (\gamma I(i) - \mu R(i-1) + uI(i))h^\alpha - \sum_{j=1}^i c(j)R(i-j), \\
 B(i) &= (\sigma I(i) - dB(i-1))h^\alpha - \sum_{j=1}^i c(j)B(i-j),
 \end{aligned}$$

where $c(0) = 1$ and $c(j) = (1 - (1 + \alpha)/j)c_{j-1}$, $j \geq 1$, and h^α is the time step size. The last term in the above system of equations stands for memory.

The system of the adjoint variables is solved using the following iterative scheme:

$$\begin{aligned}
 p_1(i) &= (p_1(i-1)(\beta_h I(i) + \beta_e B(i) + \mu) - p_2(i-1)(\beta_h I(i) + \beta_e B(i)))h^\alpha \\
 &\quad - \sum_{j=1}^i (c(j), p_1(i-j)), \\
 p_2(i) &= (-C_1 + p_1(i)\beta_h S(i) - p_2(i-1)\beta_h S(i) + p_2(i-1)(\gamma + \mu + \delta + u) \\
 &\quad - p_3(i-1)(\gamma + u) - p_4(i-1)\sigma)h^\alpha - \sum_{j=1}^i (c(j), p_2(i-j)), \\
 p_3(i) &= (p_3(i-1)\mu)h^\alpha - \sum_{j=1}^i (c(j), p_3(i-j)), \\
 p_4(i) &= (p_4(i-1)d + p_1(i)\beta_e S(i) - p_2(i)\beta_e S(i))h^\alpha - \sum_{j=1}^i (c(j), p_4(i-j)).
 \end{aligned}$$

The value of the optimal control is updated using the following scheme:

$$u(t) = \max \left\{ \min \left\{ \frac{(p_2(i) - p_3(i))I(i)}{2C_2}, 1 \right\}, 0 \right\}. \quad (5)$$

First, for DFE, we choose $A = 0.5$, $\beta_h = 0.1$, $\beta_e = 0.3$, $\mu = 0.1$, $\delta = 0.2$, $\gamma = 0.6$, $\sigma = 0.01$, $d = 0.7$. For these values of the parameters, we get $R_0 = 0.579365$, and the DFE is $(5, 0, 0)$. The local stability of the DFE is shown in the following Fig. 3. Now we take the same values of the parameters as earlier and choose $\alpha = 0.92$. In this case, also we have $R_0 = 0.579365 < 1$, and we observe that all the solution curves of the system with different initial values converge to the point $E_0(5, 0, 0)$ (Fig. 4). This establishes the global asymptotic stability of the infection-free fixed point. Biologically, global stability of the disease-free equilibrium indicates that the system can be made free from the disease if we can achieve the specified condition.

For the endemic state, we choose the parameters values as $A = 6$, $\beta_h = 0.08$, $\beta_e = 0.3$, $\mu = 0.3$, $\delta = 0.2$, $\gamma = 0.6$, $\sigma = 0.2$, $d = 0.7$. In this case, we obtain $R_0 = 3.01299 (> 1)$. So, there is a unique infected equilibrium as $(S^*, I^*, B^*) = (6.63793, 3.64421, 1.0412)$. Also, we note that for these values of the parameters, $r_1 = 2.17286 > 0$, $r_2 = 1.4677 > 0$, $r_3 = 0.465 > 0$ and $r_1 r_1 - r_3 = 2.72411 > 0$. Hence, it follows from Theorem 4 that the infected state is locally stable (Fig. 5). We have plotted the solution trajectories for different values of α , and we observe that the solutions trajectories converges to the steady states as fast as the fractional order $\alpha \rightarrow 1$. Figure 6 depicts that the solution curves converges to the endemic steady state starting from different initial conditions. This characterizes the global stability of the infected equilibrium point. The global stability of the endemic steady state indicates the disease persist in the community.

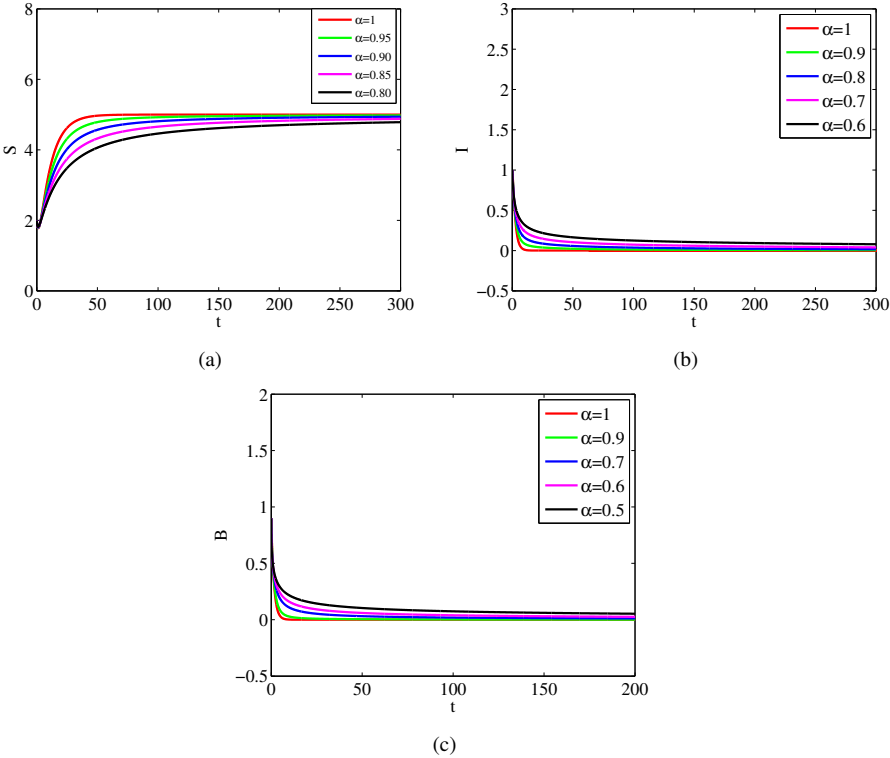


Figure 3. Time series plot showing the local stability of infection-free equilibrium.

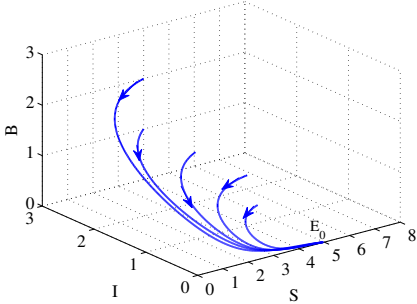


Figure 4. Phase space showing the global stability of infection free state.

To solve the fractional-order control problem numerically, we choose the values of the model parameters as $A = 64$, $\beta_e = 0.01$, $\beta_h = 0.08$, $\mu = 0.3$, $\gamma = 0.6$, $\sigma = 0.2$, $k = 0.7$, $\delta = 0.2$, $\alpha = 0.5$, $C_1 = 2$, $C_2 = 1$. In Fig. 7, we have plotted the infected populations considering with control and without control. It is noted that in the presence of the treatment control and memory, the number of infected population reduces

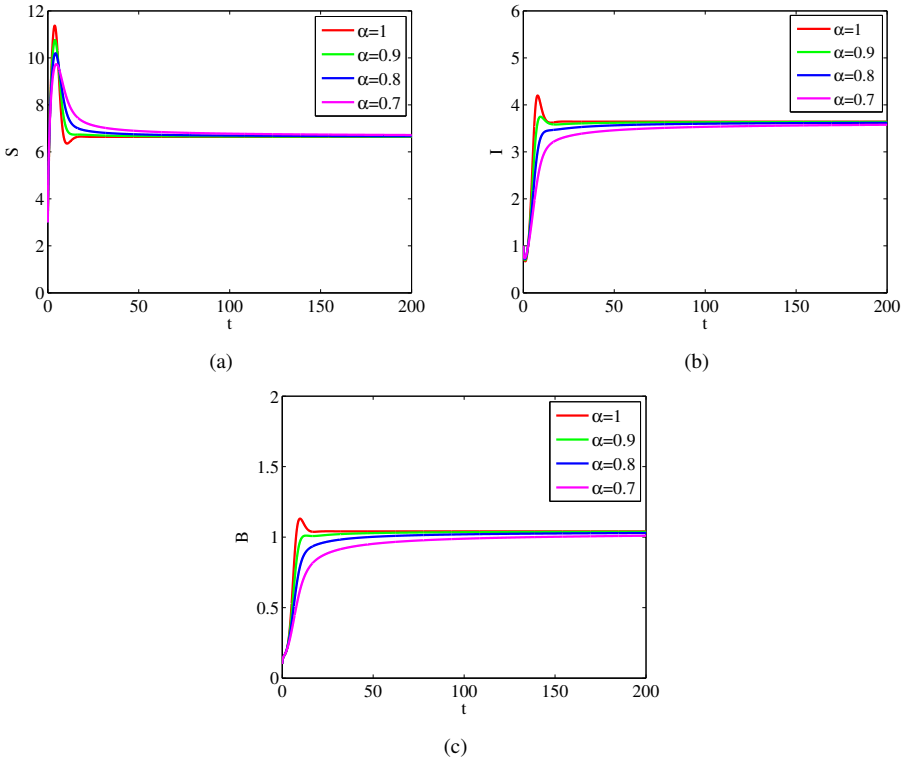


Figure 5. Time series plot showing the local asymptotic stability of the endemic steady state.

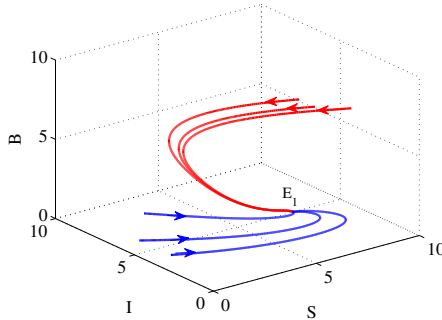


Figure 6. Phase space showing the global stability of endemic steady state.

as compared to the no control situation. So, in the presence of memory, treatment control has a positive effect on the management of the disease. Also, in Fig. 8, the variation of the treatment control with respect to time is shown. It is very interesting to note that the control profile depicts that the control should be applied when the disease prevalence become high, otherwise it should be stopped.

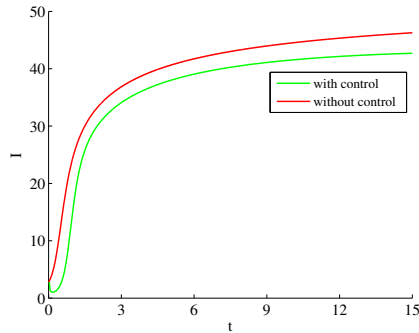


Figure 7. Effect of control on the infected populations when $\alpha = 0.5$.

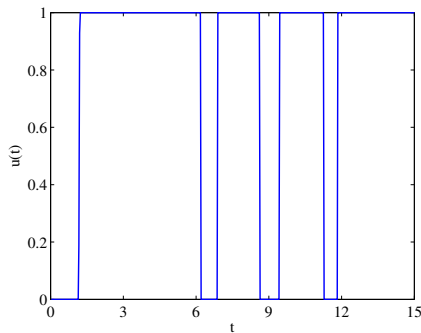


Figure 8. Variation of the treatment control with respect to time.

7 Conclusions

In this article, we have presented a cholera model with fractional-order derivative. Incorporating fractional-order derivative to any biological system make the system more realistic, and it includes more features than the traditional integer-order derivative. Fractional-order derivative allow us to model a higher-order system by a lower-order model. Furthermore, in control theory, fractional-order calculus is better than the integer-order in the sense that it is capable to handle the time-dependent impacts as noticed in the real-world process. In particular, it include the memory like behavior of the circuits.

First, we have studied the biological well-posedness of the formulated model. The expression of the epidemic threshold, i.e., basic reproduction number is derived using the next generation matrix approach. The theoretical analysis implies that the system has a infection-free equilibrium when $R_0 < 1$ and a unique infected equilibrium when $R_0 > 1$. The global asymptotic stability of both equilibrium points are established using Lyapunov technique. It is observed that the fractional order of the derivative and basic reproduction number play a crucial role in the stability behavior of the steady states.

The numerical works support the analytical results. From the numerical simulations it is evident that the solutions trajectories converge to the steady states as fast as the fractional order $\alpha \rightarrow 1$. So, we can conclude that the stability of the equilibrium points is independent of different fractional-order derivatives, while the fractional-order derivative only affects the time to reach the stationary states. Also, the simulation works of the control problem suggest that in the presence of memory, optimal application of treatment control reduces the number of infected people. Moreover, from sensitivity analysis it is found that the natural death rate and the diminishing rate of bacteria have the negative impact on R_0 . So, by controlling these two parameters and applying appropriate treatments to the infected people, it is possible to reduce the cholera prevalence. In addition to the treatment control, it will be interesting to investigate the impacts of the other control measures like vaccination, isolation, awareness program on the transmission dynamics of cholera. We left this point as our future research topic.

Conflicts of interest. The authors declare that there is no competing interests.

Acknowledgment. The authors are very much grateful to the anonymous reviewers and the editor Linas Petkevičius for their constructive comments and useful suggestions to improve the quality and presentation of the manuscript significantly.

References

1. R. Almeida, Analysis of a fractional SEIR model with treatment, *Appl. Math. Lett.*, **84**:56–62, 2018, <https://doi.org/10.1016/j.aml.2018.04.015>.
2. R. Almeida, A.M. Brito da Cruz, N. Martins, M.T.T. Monteiro, An epidemiological MSEIR model described by the Caputo fractional derivative, *Int. J. Dyn. Control*, **7**:776–784, 2019, <https://doi.org/10.1007/s40435-018-0492-1>.
3. E. Bonyah, J.F. Gómez-Aguilar, A. Adu, Stability analysis and optimal control of a fractional human African trypanosomiasis model, *Chaos Solitons Fractals*, **117**:150–160, 2018, <https://doi.org/10.1016/j.chaos.2018.10.025>.
4. D.K. Das, A. Khatua, T.K. Kar, S. Jana, The effectiveness of contact tracing in mitigating COVID-19 outbreak: A model-based analysis in the context of India, *Appl. Math. Comput.*, **404**:126207, 2021, <https://doi.org/10.1016/j.amc.2021.126207>.
5. K. Diethelm, N.J. Ford, Analysis of fractional differential equations, *J. Math. Anal. Appl.*, **265**(2):229–248, 2002, <https://doi.org/10.1006/jmaa.2000.7194>.
6. R. Garrappa, Trapezoidal methods for fractional differential equations: Theoretical and computational aspects, *Math. Comput. Simul.*, **110**:96–112, 2015, <https://doi.org/10.1016/j.matcom.2013.09.012>.
7. J. Huo, H. Zhao, L. Zhu, The effect of vaccines on backward bifurcation in a fractional order HIV model, *Nonlinear Anal., Real World Appl.*, **26**:289–305, 2015, <https://doi.org/10.1016/j.nonrwa.2015.05.014>.
8. A. Jajarmi, D. Baleanu, A new fractional analysis on the interaction of HIV with CD4+ T-cells, *Chaos Solitons Fractals*, **113**:221–229, 2018, <https://doi.org/10.1016/j.chaos.2018.06.009>.

9. M.J. Keeling, P. Rohani, *Modeling Infectious Diseases in Humans and Animals*, Princeton Univ. Press, Princeton, NJ, 2011.
10. W.O. Kermack, A.G. McKendrick, A contribution to the mathematical theory of epidemics, *Proc. R. Soc. Lond., Ser. A*, **115**(772):700–721, 1927, <https://doi.org/10.1098/rspa.1927.0118>.
11. A. Khatua, T.K. Kar, Dynamical behavior and control strategy of a dengue epidemic model, *Eur. Phys. J. Plus*, **135**:1–22, 2020, <https://doi.org/10.1140/epjp/s13360-020-00654-8>.
12. A. Khatua, T.K. Kar, Impacts of media awareness on a stage structured epidemic model, *Int. J. Appl. Comput. Math.*, **6**:1–22, 2020, <https://doi.org/10.1007/s40819-020-00904-4>.
13. A. Khatua, T.K. Kar, S.K. Nandi, S. Jana, Y. Kang, Impact of human mobility on the transmission dynamics of infectious diseases, *Energy Ecol. Environ.*, **5**:389–406, 2020, <https://doi.org/10.1007/s40974-020-00164-4>.
14. A.P. Lemos-Paião, C.J. Silva, D.F.M. Torres, An epidemic model for cholera with optimal control treatment, *J. Comput. Appl. Math.*, **318**:168–180, 2017, <https://doi.org/10.1016/j.cam.2016.11.002>.
15. H.L. Li, L. Zhang, C. Hu, Y.L. Jiang, Z. Teng, Dynamical analysis of a fractional-order predator-prey model incorporating a prey refuge, *J. Appl. Math. Comput.*, **54**:435–449, 2017, <https://doi.org/10.1007/s12190-016-1017-8>.
16. C. Lubich, Discretized fractional calculus, *SIAM J. Math. Anal.*, **17**(3):704–719, 1986, <https://doi.org/10.1137/0517050>.
17. S. Majee, S. Jana, D.K. Das, T.K. Kar, Global dynamics of a fractional-order HFMD model incorporating optimal treatment and stochastic stability, *Chaos Solitons Fractals*, **161**:112291, 2022, <https://doi.org/10.1016/j.chaos.2022.112291>.
18. M. Mandal, S. Jana, S. Adak, A. Khatua, T.K. Kar, A model-based analysis to predict and control the dynamics of COVID-19, in A.T. Azar, A.E. Hassanien (Eds.), *Modeling, Control and Drug Development for COVID-19 Outbreak Prevention*, Stud. Syst. Decis. Control, Vol. 366, Springer, Cham, 2022, pp. 87–118, https://doi.org/10.1007/978-3-030-72834-2_4.
19. S. Mondal, A. Lahiri, N. Bairagi, Analysis of a fractional order eco-epidemiological model with prey infection and type 2 functional response, *Math. Methods Appl. Sci.*, **40**(18):6776–6789, 2017, <https://doi.org/10.1002/mma.4490>.
20. A. Mouaouine, A. Boukhouima, K. Hattaf, N. Yousfi, A fractional order SIR epidemic model with nonlinear incidence rate, *Adv. Differ. Equ.*, **2018**(1):160, 2018, <https://doi.org/10.1186/s13662-018-1613-z>.
21. D. Mukherjee, L.N. Guin, S. Chakravarty, A reaction–diffusion mathematical model on mild atherosclerosis, *Model. Earth Syst. Environ.*, **5**:1853–1865, 2019, <https://doi.org/10.1007/s40808-019-00643-6>.
22. P.A. Naik, J. Zu, K.M. Owolabi, Global dynamics of a fractional order model for the transmission of HIV epidemic with optimal control, *Chaos Solitons Fractals*, **138**:109826, 2020, <https://doi.org/10.1016/j.chaos.2020.109826>.
23. Z.M. Odibat, N.T. Shawagfeh, Generalized Taylor’s formula, *Appl. Math. Comput.*, **186**(1):286–293, 2007, <https://doi.org/10.1016/j.amc.2006.07.102>.

24. I. Podlubny, *Fractional Differential Equations*, Math. Sci. Eng., Vol. 198, Academic Press, SanDiego, CA, 1999.
25. L.S. Pontryagin, V.G. Boltyanskiy, R.V. Gamkrelidze, E.F. Mishchenko, *Mathematical Theory of Optimal Processes*, Wiley, New York, 1962.
26. S. Rosa, D.F.M. Torres, Optimal control and sensitivity analysis of a fractional order TB model, *Stat. Optim. Inf. Comput.*, **7**(3):617–625, 2019, <https://doi.org/10.19139/soic.v7i3.836>.
27. G.Q. Sun, J.H. Xie, S.H. Huang, Z. Jin, M.T. Li, L. Liu, Transmission dynamics of cholera: Mathematical modeling and control strategies, *Commun. Nonlinear Sci. Numer. Simul.*, **45**: 235–244, 2017, <https://doi.org/10.1016/j.cnsns.2016.10.007>.
28. J.P. Tian, J. Wang, Global stability for cholera epidemic models, *Math. Biosci.*, **232**(1):31–41, 2011, <https://doi.org/10.1016/j.mbs.2011.04.001>.
29. P. Van den Driessche, J. Watmough, Reproduction numbers and sub-threshold endemic equilibria for compartmental models of disease transmission, *Math. Biosci.*, **180**(1–2):29–48, 2002, [https://doi.org/10.1016/S0025-5564\(02\)00108-6](https://doi.org/10.1016/S0025-5564(02)00108-6).
30. C. Vargas-De-León, Volterra-type Lyapunov functions for fractional-order epidemic systems, *Commun. Nonlinear Sci. Numer. Simul.*, **24**(1-3):75–85, 2015, <https://doi.org/10.1016/j.cnsns.2014.12.013>.
31. X. Wang, D. Gao, J. Wang, Influence of human behavior on cholera dynamics, *Math. Biosci.*, **267**:41–52, 2015, <https://doi.org/10.1016/j.mbs.2015.06.009>.
32. W. Wojtak, C.J. Silva, D.F.M. Torres, Uniform asymptotic stability of a fractional tuberculosis model, *Math. Model. Nat. Phenom.*, **13**(1):9, 2018, <https://doi.org/10.1051/mmnp/2018015>.
33. X. Zhou, J. Cui, Modeling and stability analysis for a cholera model with vaccination, *Math. Methods Appl. Sci.*, **34**(14):1711–1724, 2011, <https://doi.org/10.1002/mma.1477>.
34. X. Zhou, X. Shi, J. Cui, Stability and backward bifurcation on a cholera epidemic model with saturated recovery rate, *Math. Methods Appl. Sci.*, **40**(4):1288–1306, 2017, <https://doi.org/10.1002/mma.4053>.
35. <https://www.who.int/news-room/fact-sheets/detail/cholera>.